

# Effective Generation of Feasible Solutions for Integer Programming via Guided Diffusion

Hao Zeng  
zenghao.zeng@cainiao.com  
Cainiao Network  
Hangzhou, China

Jiaqi Wang  
tangqiao.wjq@cainiao.com  
Cainiao Network  
Hangzhou, China

Avirup Das  
avirup.das@postgrad.manchester.ac.uk  
University of Manchester  
Manchester, United Kingdom

Junying He  
junying.hjy@cainiao.com  
Cainiao Network  
Hangzhou, China

Kunpeng Han  
Haoyuan Hu  
kunpeng.hkp@cainiao.com  
haoyuan.huhu@cainiao.com  
Cainiao Network  
Hangzhou, China

Mingfei Sun\*  
mingfei.sun@manchester.ac.uk  
University of Manchester  
Manchester, United Kingdom

## ABSTRACT

Feasible solutions are crucial for Integer Programming (IP) since they can substantially speed up the solving process. In many applications, similar IP instances often exhibit similar structures and shared solution distributions, which can be potentially modeled by deep learning methods. Unfortunately, existing deep-learning-based algorithms, such as Neural Diving [21] and Predict-and-search framework [8], are limited to generating only partial feasible solutions, and they must rely on solvers like SCIP and Gurobi to complete the solutions for a given IP problem. In this paper, we propose a novel framework that generates *complete* feasible solutions *end-to-end*. Our framework leverages contrastive learning to characterize the relationship between IP instances and solutions, and learns latent embeddings for both IP instances and their solutions. Further, the framework employs diffusion models to learn the distribution of solution embeddings conditioned on IP representations, with a dedicated guided sampling strategy that accounts for both constraints and objectives. We empirically evaluate our framework on four typical datasets of IP problems, and show that it effectively generates complete feasible solutions with a high probability ( $> 89.7\%$ ) without the reliance of Solvers and the quality of solutions is comparable to the best heuristic solutions from Gurobi. Furthermore, by integrating our method's sampled partial solutions with the CompleteSol heuristic from SCIP [19], the resulting feasible solutions outperform those from state-of-the-art methods across all datasets, exhibiting a 3.7 to 33.7% improvement in the gap to optimal values, and maintaining a feasible ratio of over 99.7% for all datasets.

\*Corresponding author.

## CCS CONCEPTS

• **Computing methodologies** → *Neural networks; Learning in probabilistic graphical models; Machine learning approaches.*

## KEYWORDS

Integer Programming, Diffusion Models

## ACM Reference Format:

Hao Zeng, Jiaqi Wang, Avirup Das, Junying He, Kunpeng Han, Haoyuan Hu, and Mingfei Sun. 2024. Effective Generation of Feasible Solutions for Integer Programming via Guided Diffusion. In *Proceedings of the 30th ACM SIGKDD Conference on Knowledge Discovery and Data Mining (KDD '24)*, August 25–29, 2024, Barcelona, Spain. ACM, New York, NY, USA, 12 pages. <https://doi.org/10.1145/3637528.3671783>

## 1 Introduction

Integer Programming (IP) in the field of operation research is a class of optimization problems where some or all of the decision variables are constrained to be integers [36]. Despite their importance in a wide range of applications such as production planning [25, 30], resource allocation [12], and scheduling [23, 29, 35], IP is known to be NP-hard and in general very difficult to solve. For decades, a significant effort has been made to develop sophisticated algorithms and efficient solvers, e.g., branch-and-bound [16], cutting plane method [13] and large neighborhood search algorithms [24]. These methods, however, can be computationally expensive because the search space for large-scale problems can be exponentially large. Moreover, these algorithms rely heavily on a feasible solution input that will crucially determine the whole search process. Consequently, existing solvers, such as SCIP [19] and Gurobi [7], firstly employ heuristic algorithms to identify high-quality feasible solutions that serve as initial starting points for the optimization process. However, the heuristic algorithms usually fail to capture the similar structure among different IP instances and the quality of initial solutions is usually low. Hence, having a data-driven method that produces high-quality feasible solutions for any IP instances is desirable for many real-world applications.

To generate feasible solutions, prior works [8, 21, 38] have employed the advantage of deep learning to capture similarity of the IP instances from the same domain in order to expedite solving. For



This work is licensed under a Creative Commons Attribution-NonDerivs International 4.0 License.

presenting IP instances via neural network, Neural Diving [21, 38] adopt the methodology delineated by Gasse et al. [5], which models the formulation of IP instances as bipartite graphs and subsequently leveraging Graph Neural Networks (GNN) to derive variable features from these graph representations. Subsequently, a solution prediction task is employed to learn the relationship between IP instances and their solutions, with the aim of directly predicting those solutions. However, it is difficult to produce complete feasible solutions as it fails to explicitly integrate objective and constraint information during the sampling process. Neural Diving thus focus on generating partial solutions by GNN, where only a subset of variables is assigned values using neural networks. Importantly, in many cases, the proportion of variables predicted by the neural network is set at a relatively low ratio (less than 50%) to ensure feasibility. Furthermore, such methods tend to be inefficient, primarily due to the introduction of auxiliary problems for filling in the remaining variables. For instance, the Completesol heuristic [19], a classical approach, solves an auxiliary integer programming model which is constructed by adding constraints to fix the variables from partial solutions. Nonetheless, infeasibility can arise in auxiliary problems due to the potential for partial assignments to clash with the initial constraints. To deal with infeasible assignments, in another approach, Han et al. [8] proposes a predict-and-search algorithm which constructs a trust region based on predicted partial solutions and then search for high-quality feasible solutions via a solver. In summary, these methods require the construction of auxiliary problems to obtain feasible solutions and fail to utilize the complete information from the IP instance, as only partial variables are assigned. This situation highlights the necessity for creating an end-to-end deep learning framework capable of generating complete and feasible solutions for IP problems.

Recently, diffusion models [9, 31] have exhibited notable advantages in various generative tasks, primarily owing to their superior mode-coverage and diversity [2]. Notable applications include high-fidelity image generation [4], image-segmentation [1], and text-to-image synthesis [28]. These successes motivates the launch of an investigation into harnessing the generative capability of diffusion models for acquiring feasible solutions of IP problems.

To this end, we introduce a comprehensive end-to-end generative framework presented in Figure 1 to produce high-quality feasible solutions for IP problems. First of all, stemming inspiration from DALLE-2 [28] for text-to-image translation, we employ a multimodal contrastive learning approach, akin to the CLIP Algorithm [27], to obtain embeddings for an IP instance  $i$ , denoted as  $\mathbf{z}_i$ , and solution embeddings  $\mathbf{z}_x$  for solutions  $\mathbf{x}$  (Section 3). Subsequently, we employ DDPM [9] to model the distribution of  $\mathbf{z}_x$  conditioned on  $\mathbf{z}_i$  (Section 3). During this phrase, a decoder is concurrently trained with the task of solution reconstruction (Section 3). Finally, to enhance the quality of the feasible solutions during the sampling process, we propose the IP-guided sampling approaches tailored for both DDPM and DDIM [33] which explicitly consider both constraints and objectives during sampling. Our experimental results shown in Section 5 substantiate the efficacy of this approach in generating complete and feasible solutions for a given IP instance with a higher probability. Besides, by combining with the CompleteSol heuristic, the solutions from our methods have better quality than the state-of-the-art. Importantly, to the best of our

knowledge, our approach is the first to have the ability to generate complete and feasible solutions using *pure* neural techniques, without relying on any solvers.

## 2 Background

**Integer Programming and Its Representations.** Integer programming (IP) is a class of NP-hard problems where the goal is to optimize a linear objective function, subject to linear and integer constraints. Without loss of generality, we focus on minimization which can be formulated as follows,

$$\min_{\mathbf{x}} \mathbf{c}^\top \mathbf{x} \quad \text{subject to } \mathbf{A}\mathbf{x} \leq \mathbf{b}, \quad \mathbf{x} \in \mathbb{Z}^n \quad (1)$$

where  $\mathbf{c} \in \mathbb{R}^n$  denotes the objective coefficient,  $\mathbf{A} = [\mathbf{a}_1^\top, \mathbf{a}_2^\top, \dots, \mathbf{a}_m^\top] \in \mathbb{R}^{m \times n}$  is the coefficient matrix of constraints and  $\mathbf{b} = [b_1, b_2, \dots, b_m]^\top \in \mathbb{R}^m$  represents the right-hand-side vector. For simplicity, we focus on binary integer variables, where  $\mathbf{x}$  takes values in  $\{0, 1\}^n$ . Throughout this paper, we adopt the term *IP instance* to denote a specific instance within the domain of some Integer Programming (IP) problem.

Bipartite graph representation, proposed by Gasse et al. [5], is a commonly used and useful way to extract features of an IP instance for machine learning purposes. This representation, see the left part of Figure 1 (a) for an example, divides the constraints and variables into two different sets of nodes, and uses a Graph Convolution Network (GCN) to learn the representation of nodes. Recently, Nair et al. [21] proposed several changes to the architecture of GCN for performance improvements. Therefore, in this work, we use the bipartite graph structure combined with GCN to extract the embeddings of IP instances (see [5, 21] for more details).

**DDPM and DDIM.** Diffusion models learn a data distribution by reversing a gradual noising process. In the DDPM method [9], when presented with a data point sampled from an actual data distribution, denoted as  $\mathbf{z}_x^{(0)} \sim q(\mathbf{z}_x)$ , a diffusion model, as described in [9, 31], typically involves two distinct phases. In the forward process, a sequence of Gaussian noise is incrementally added to the initial sample over a span of  $T$  steps, guided by a variance schedule denoted as  $\beta_1, \beta_2, \dots, \beta_T$ . This process yields a sequence of noisy samples  $\mathbf{z}_x^{(1)}, \mathbf{z}_x^{(2)}, \dots, \mathbf{z}_x^{(T)}$ . Subsequently, the transition for the forward process can be described as:  $q(\mathbf{z}_x^{(t)} | \mathbf{z}_x^{(t-1)}) = \mathcal{N}(\mathbf{z}_x^{(t)}; \sqrt{1 - \beta_t} \mathbf{z}_x^{(t-1)}, \beta_t \mathbf{I})$ . In fact,  $\mathbf{z}_x^{(t)}$  can be sampled at any time step  $t$  in a closed form employing the notations  $\alpha_t := 1 - \beta_t$  and  $\bar{\alpha} := \prod_{s=1}^t \alpha_s$ ,  $\mathbf{z}_x^{(t)} = \sqrt{\bar{\alpha}_t} \mathbf{z}_x^{(0)} + \sqrt{1 - \bar{\alpha}_t} \epsilon$ , where  $\epsilon \sim \mathcal{N}(0, \mathbf{I})$ . In the reverse process (denoising process), we need to model the distribution of  $\mathbf{z}_x^{(t-1)}$  given  $\mathbf{z}_x^{(t)}$  as a Gaussian distribution, which implies that  $p_\theta(\mathbf{z}_x^{(t-1)} | \mathbf{z}_x^{(t)}) = \mathcal{N}(\mathbf{z}_x^{(t-1)}; \boldsymbol{\mu}_\theta(\mathbf{z}_x^{(t)}, t), \Sigma_\theta(\mathbf{z}_x^{(t)}, t))$ , where the variance  $\Sigma_\theta(\mathbf{z}_x^{(t)}, t)$  can be fixed to a known constant [9] or learned with a separate neural network [22], while the mean can be approximately computed by adding  $\mathbf{z}_x^{(0)}$  as a condition,  $\boldsymbol{\mu}_\theta(\mathbf{z}_x^{(t)}, t) = \frac{\sqrt{\bar{\alpha}_t}(1 - \bar{\alpha}_{t-1})}{1 - \bar{\alpha}_t} \mathbf{z}_x^{(t)} + \frac{\sqrt{\bar{\alpha}_{t-1}}\beta_t}{1 - \bar{\alpha}_t} \mathbf{z}_x^{(0)}$ .

To improve the efficiency of sampling of DDPM, DDIM [33] formulates an alternative non-Markovian noising process with the same forward marginals as DDPM, but rewrites the probability  $p_\theta(\mathbf{z}_x^{(t-1)} | \mathbf{z}_x^{(t)})$  in reverse process as a desired standard deviation

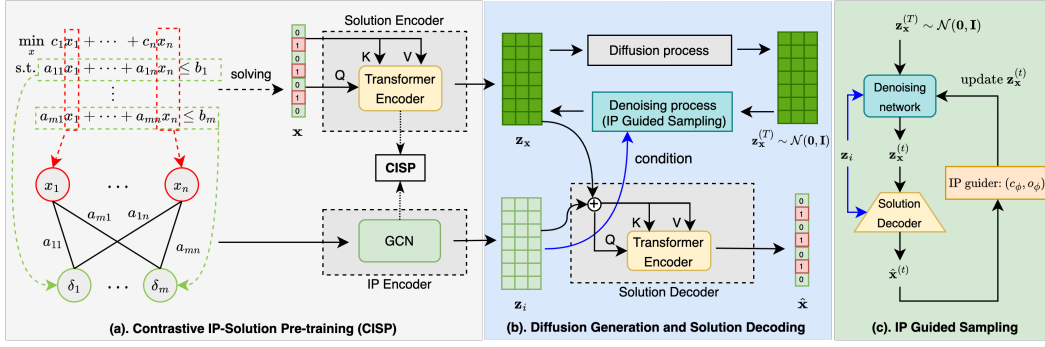


**Figure 1: Our method first trains the IP Encoder and Solution Encoder to acquire the IP embedding ( $z_i$ ) and Solution embedding ( $z_x$ ) using CISP. We then jointly train diffusion models and the solution decoder to capture the distribution of solutions given a specific IP instance. In the sampling stage, we employ an IP guided diffusion sampling to account for both the objective and constraints.**

$\sigma_t$ . DDIM then derives the following distribution in the reverse process,

$$q_{\sigma}(z_x^{(t-1)} | z_x^{(t)}, z_x^{(0)}) = \mathcal{N}\left(z_x^{(t-1)}; \sqrt{\bar{\alpha}_t} z_x^{(0)} + \sqrt{1 - \bar{\alpha}_t - \sigma_t^2} \epsilon^{(t)}, \sigma_t^2 \mathbf{I}\right), \quad (2)$$

where  $\epsilon^{(t)} = (z_x^{(t)} - \sqrt{\bar{\alpha}_t} z_x^{(0)}) / (1 - \bar{\alpha}_t)$  shows the direction to  $z_x^{(t)}$ .

### 3 Model Architecture

Our training dataset consists of pairs  $(i, \mathbf{x})$  of IP instance and their corresponding one feasible solution  $\mathbf{x}$ . Given an instance  $i$ , let  $z_i \in \mathbb{R}^{n \times d}$  and  $z_x \in \mathbb{R}^{n \times d}$  be the embeddings of the IP instance  $i$  and the solution  $\mathbf{x}$  respectively, where  $n$  is the number of variables and  $d$  is the embedding dimension. It is worth noting that a IP instance can have multiple different feasible solutions, meaning that model need to learn the distribution of feasible solutions by conditioning on a given IP instance. Our methods do not directly apply a diffusion model to learn the distribution of solutions. Instead, we use an encoder to transform the solutions  $\mathbf{x} \in \{0, 1\}^n$  from a discrete space to a continuous embedding space, e.g.  $z_x \in \mathbb{R}^{n \times d}$ . We then construct a diffusion model to learn the distribution of the solution embeddings given an IP embedding  $z_i$ . Finally, a decoder is trained to recover the predicted solution  $\hat{\mathbf{x}}$  from the embedding  $z_x$ . To effectively build the connection between the IP instance  $i$  and solution  $\mathbf{x}$ , we first apply Contrastive IP-Solution Pre-training (CISP) module, motivated by CLIP [27] which is used for text-to-image generation, to produce IP embedding  $z_i$  and solution embedding  $z_x$ . Overall, our model consists of three key components:

- a *Contrastive IP-Solution Pre-training (CISP) module* that produces IP embeddings  $z_i$  and solution embeddings  $z_x$ ;
- a *diffusion module*  $p(z_x | z_i)$  that generates solution embedding  $z_x$  conditioned on IP embedding  $z_i$ ;
- and a *decoder module*  $p(\mathbf{x} | z_x, z_i)$  that recovers solution  $\mathbf{x}$  from embedding  $z_x$  conditioned on IP embedding  $z_i$ .

We provide more details on each module in the following sections.

**Contrastive IP-Solution Pre-training.** Previous works [8, 21] show the crucial importance of establishing the connection between the IP instances and the solutions, and propose to implicitly learn this connection through the task of predicting feasible solutions. These approaches may not exhibit strong generalization capabilities on new instances because they only utilize the collected solutions in dataset without considering feasibility explicitly during training. To more effectively capture this relationship, we propose to employ a contrastive learning task to learn representations for IP instances and embeddings for solutions by constructing feasible and infeasible solutions. The intuition behind is to ensure that the IP embeddings stay close to the embeddings of their feasible solutions, and away from the embeddings of the infeasible ones. To avoid explicitly constructing infeasible solutions, we proposed Contrastive IP-Solution Pre-training (CISP) algorithm to train IP encoder and solution encoder. Specifically, for IP encoder, we extract the representation of IP instances via a bipartite graph as [5], and use the structure of GCNs from Neural Diving [21] to generate all variables' embeddings as IP embeddings  $z_i$ . For solution encoder, we use the encoder of the transformer to obtain the representations of each variable as solution embeddings  $z_x$ . Both  $z_x$  and  $z_i$  have the same dimension to compute pairwise cosine similarities later. Since the number of variables in different IP instances may vary, we perform zero-padding on  $z_i$  and dummy-padding on  $\mathbf{x}$  (i.e. padding 2 for 0-1 integer programming) to align the dimensions. The zero-padding for  $z_i$  is done to ensure that the cosine similarity remains unaffected. CISP algorithm then learns to maximize the similarity between embeddings of IP and corresponding solution pairs, and to minimize the similarity between the embeddings of incorrect pairs, which is achieved through optimizing a symmetric cross-entropy loss, as detailed in Appendix A.1.

**Diffusion Generation.** To leverage diffusion models for generating feasible solutions (discrete variables), we use the solution embedding  $z_x \in \mathbb{R}^{n \times d}$  from the aforementioned CISP as the objective of generation. In addition,  $z_i$  is considered as a condition for

generating high-quality results. According to [9], we parameterize

$$p_{\theta}(\mathbf{z}_x^{(t-1)} | \mathbf{z}_x^{(t)}, \mathbf{z}_i) = \mathcal{N}\left(\mathbf{z}_x^{(t-1)}; \boldsymbol{\mu}_{\theta}(\mathbf{z}_x^{(t)}, \mathbf{z}_i, t), \boldsymbol{\Sigma}_{\theta}(\mathbf{z}_x^{(t-1)}, \mathbf{z}_i, t)\right), \quad (3)$$

$\forall t \in [T, T-1, \dots, 1]$  in reverse process, where  $\mathbf{z}_x^{(0)} = \mathbf{z}_x$ . Different from predicting the noise of each step in a general diffusion training phase, we predict  $\mathbf{z}_x$  directly as it empirically performs better. The training loss is defined as follows,

$$\mathcal{L}_{\text{MSE}} \triangleq \mathbb{E}_{t, \mathbf{z}_x^{(t)}} \left[ \|\mathbf{f}_{\theta}(\mathbf{z}_x^{(t)}, \mathbf{z}_i, t) - \mathbf{z}_x\|^2 \right], \quad (4)$$

where  $\mathbf{f}_{\theta}$  is an encoder-based transformer model with specific structure shown in Figure 2 and  $\mathbf{z}_x^{(t)} = \sqrt{\bar{\alpha}_t} \mathbf{z}_x + \sqrt{1 - \bar{\alpha}_t} \boldsymbol{\epsilon}^{(t)}$ ,  $\boldsymbol{\epsilon}^{(t)} \sim \mathcal{N}(\mathbf{0}, \mathbf{I})$ .

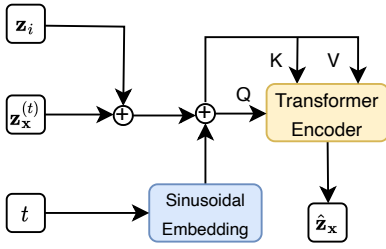


Figure 2: Diffusion model  $\mathbf{f}_{\theta}(\mathbf{z}_x^{(t)}, \mathbf{z}_i, t)$

**Solution Decoding.** The decoder  $\mathbf{d}_{\phi}$  plays a crucial role in reconstructing the solution  $\mathbf{x}$  from the solution embedding  $\mathbf{z}_x$ . To enhance the robustness of the solution recovery, we jointly train the decoder  $\mathbf{d}_{\phi}$  with the diffusion model. Specifically, we concatenate the solution embedding  $\hat{\mathbf{z}}_x = \mathbf{f}_{\theta}(\mathbf{z}_x^{(t)}, \mathbf{z}_i, t)$  generated by the diffusion model with the IP embedding  $\mathbf{z}_i$ , and use the concatenated vector as input to a transformer encoder to obtain the reconstructed solution  $\hat{\mathbf{x}} = \mathbf{d}_{\phi}(\hat{\mathbf{z}}_x, \mathbf{z}_i)$ . This process is associated with the cross-entropy loss defined as:  $\mathcal{L}_{\text{CE}} \triangleq -\mathbb{E}_{\mathbf{x}} [\log \hat{\mathbf{x}}] = -\mathbb{E}_{\mathbf{x}} [\log \mathbf{d}_{\phi}(\hat{\mathbf{z}}_x, \mathbf{z}_i)]$ . To explicitly account for constraints in the training process, we introduce a penalty term to measure the degree of constraint violation. More specifically, let  $\mathbf{a}_k^T$  be the  $k$ th row of matrix  $\mathbf{A}$  in (1), the constraint violation (CV) loss is defined as  $\mathcal{L}_{\text{CV}} \triangleq \frac{1}{m} \sum_{k=1}^m \max(\mathbf{a}_k^T \hat{\mathbf{x}} - b_k, 0)$ , where  $m$  is the number of constraints. The total loss for training diffusion and decoder therefore consists of the three parts:

$$\mathcal{L} = \mathcal{L}_{\text{MSE}} + \mathcal{L}_{\text{CE}} + \lambda \mathcal{L}_{\text{CV}}, \quad (5)$$

where  $\lambda$  is a hyper-parameter to regulate the penalty. The full training procedure is given in Algorithm 1 and the training details can be found in Appendix A.4.

## 4 IP Guided Sampling

Once the models have been trained, we can then sample variable assignments by running the sampling algorithm of DDPM or DDIM from a random Gaussian noise  $\mathbf{z}_x^{(T)} \sim \mathcal{N}(\mathbf{0}, \mathbf{I})$ . Interestingly we find that, without suitable guidance, diffusion model is prone to generate inaccurate distributions, e.g. violating constraints for a given IP instance as shown in section 5.1. We thus consider the

---

### Algorithm 1 Training diffusion and solution decoder

---

**Input:** IP instance embedding  $\mathbf{z}_i$  from CISP, solution embedding  $\mathbf{z}_x$  from CISP  
**Require:** diffusion model  $\mathbf{f}_{\theta}$ , and solution decoder  $\mathbf{d}_{\phi}$ .

- 1: **repeat**
- 2:    $t \sim \text{Uniform}(\{1, \dots, T\})$
- 3:    $\boldsymbol{\epsilon} \sim \mathcal{N}(\mathbf{0}, \mathbf{I})$
- 4:    $\hat{\mathbf{z}}_x \leftarrow \mathbf{f}_{\theta}(\sqrt{\bar{\alpha}_t} \mathbf{z}_x + \sqrt{1 - \bar{\alpha}_t} \boldsymbol{\epsilon}, \mathbf{z}_i, t)$  // predicted  $\hat{\mathbf{z}}_x$
- 5:    $\hat{\mathbf{x}} \leftarrow \mathbf{d}_{\phi}(\hat{\mathbf{z}}_x, \mathbf{z}_i)$  // reconstructed solution  $\hat{\mathbf{x}}$
- 6:   Take gradient descent step to minimize total loss in (5)
- 7: **until** Reaches a fixed number epochs or satisfies an early stopping criteria

---

constraints information  $(\mathbf{A}, \mathbf{b})$  and objective coefficient  $\mathbf{c}$  during sampling. We present the IP guided diffusion sampling for both DDPM and DDIM, of which the latter is faster and better in terms of the quality and feasibility, as shown in Section 5.

### 4.1 IP Guided Diffusion Sampling

Consider a conditional diffusion model  $p_{\theta}(\mathbf{z}_x^{(t)} | \mathbf{z}_x^{(t+1)}, \mathbf{z}_i)$ , we first introduce *constraint guidance* by designing each transition probability as

$$p_{\theta, \phi}(\mathbf{z}_x^{(t)} | \mathbf{z}_x^{(t+1)}, \mathbf{z}_i, \mathbf{A}, \mathbf{b}) = Z p_{\theta}(\mathbf{z}_x^{(t)} | \mathbf{z}_x^{(t+1)}, \mathbf{z}_i) e^{-s c_{\phi}(\mathbf{z}_x^{(t)}, \mathbf{z}_i, \mathbf{A}, \mathbf{b})}, \quad (6)$$

where  $s$  is the gradient scale,  $Z$  is a normalizing constant and  $c_{\phi}(\mathbf{z}_x^{(t)}, \mathbf{z}_i, \mathbf{A}, \mathbf{b}) = \sum_{k=1}^m \max(\mathbf{a}_k^T \mathbf{d}_{\phi}(\mathbf{z}_x^{(t)}, \mathbf{z}_i) - b_k, 0)$  measures the violation of constraints. Let  $\boldsymbol{\mu}$  and  $\boldsymbol{\Sigma}$  be the mean and variance of the Gaussian distribution representing  $p_{\theta, \phi}(\mathbf{z}_x^{(t)} | \mathbf{z}_x^{(t+1)}, \mathbf{z}_i)$ . Then,  $\log p_{\theta}(\mathbf{z}_x^{(t)} | \mathbf{z}_x^{(t+1)}, \mathbf{z}_i) = -\frac{1}{2}(\mathbf{z}_x^{(t)} - \boldsymbol{\mu})^T \boldsymbol{\Sigma}^{-1}(\mathbf{z}_x^{(t)} - \boldsymbol{\mu}) + C$ , where  $C$  is a constant. Consider the Taylor expansion for  $c_{\phi}$  at  $\mathbf{z}_x^{(t)} = \boldsymbol{\mu}$ ,

$$\begin{aligned} c_{\phi}(\mathbf{z}_x^{(t)}, \mathbf{z}_i, \mathbf{A}, \mathbf{b}) &\approx c_{\phi}(\boldsymbol{\mu}, \mathbf{z}_i, \mathbf{A}, \mathbf{b}) + (\mathbf{z}_x^{(t)} - \boldsymbol{\mu})^T \nabla_{\mathbf{z}_x^{(t)}} c_{\phi}(\mathbf{z}_x^{(t)}, \mathbf{z}_i, \mathbf{A}, \mathbf{b}) \Big|_{\mathbf{z}_x^{(t)} = \boldsymbol{\mu}} \\ &= (\mathbf{z}_x^{(t)} - \boldsymbol{\mu})^T \mathbf{g} + C_1, \end{aligned}$$

where  $\mathbf{g} = \nabla_{\mathbf{z}_x^{(t)}} c_{\phi}(\mathbf{z}_x^{(t)}, \mathbf{z}_i, \mathbf{A}, \mathbf{b}) \Big|_{\mathbf{z}_x^{(t)} = \boldsymbol{\mu}}$  and  $C_1$  is a constant. Similar to Classifier Guidance [4], we assume that  $c_{\phi}(\mathbf{z}_x^{(t)}, \mathbf{z}_i, \mathbf{A}, \mathbf{b})$  has low curvature compared to  $\boldsymbol{\Sigma}^{-1}$  and thus have the following,

$$\begin{aligned} \log(p_{\theta, \phi}(\mathbf{z}_x^{(t)} | \mathbf{z}_x^{(t+1)}, \mathbf{z}_i, \mathbf{A}, \mathbf{b})) &\approx -\frac{1}{2}(\mathbf{z}_x^{(t)} - \boldsymbol{\mu})^T \boldsymbol{\Sigma}^{-1}(\mathbf{z}_x^{(t)} - \boldsymbol{\mu}) - s(\mathbf{z}_x^{(t)} - \boldsymbol{\mu})^T \mathbf{g} + sC_1 + C_2 \\ &= -\frac{1}{2}(\mathbf{z}_x^{(t)} - \boldsymbol{\mu} + s\boldsymbol{\Sigma}\mathbf{g})^T \boldsymbol{\Sigma}^{-1}(\mathbf{z}_x^{(t)} - \boldsymbol{\mu} + s\boldsymbol{\Sigma}\mathbf{g}) + C_3, \end{aligned}$$

where  $C_3$  is a constant and can be safely ignored. Therefore, the denoising transition  $p_{\theta, \phi}(\mathbf{z}_x^{(t)} | \mathbf{z}_x^{(t+1)}, \mathbf{z}_i, \mathbf{A}, \mathbf{b})$  can be approximated by a Gaussian distribution with a mean shifted by  $-s\boldsymbol{\Sigma}\mathbf{g}$ . We can further inject the objective guidance to transition probability for acquiring high-quality solutions,

$$\begin{aligned} p_{\theta, \phi}(\mathbf{z}_x^{(t)} | \mathbf{z}_x^{(t+1)}, \mathbf{z}_i, \mathbf{A}, \mathbf{b}, \mathbf{c}) &= Z p_{\theta}(\mathbf{z}_x^{(t)} | \mathbf{z}_x^{(t+1)}, \mathbf{z}_i) e^{-s((1-\gamma)c_{\phi}(\mathbf{z}_x^{(t)}, \mathbf{z}_i, \mathbf{A}, \mathbf{b}) + \gamma o_{\phi}(\mathbf{z}_x^{(t)}, \mathbf{z}_i, \mathbf{c}))}, \quad (7) \end{aligned}$$

where  $o_\phi(\mathbf{z}_x^{(t)}, \mathbf{z}_i, \mathbf{c}) = \mathbf{c}^T \mathbf{d}_\phi(\mathbf{z}_x^{(t)}, \mathbf{z}_i)$ ,  $\mathbf{c}$  is the coefficient of objective from (1), and  $\gamma \in [0, 1]$  is the leverage factor for balancing constraint and objective. The corresponding sampling method is called *IP Guided Diffusion Sampling*, as presented in Algorithm 2.

---

**Algorithm 2** IP Guided Diffusion Sampling
 

---

**Input:** gradient scale  $s$ , leverage factor  $\gamma$ , constraint information  $(\mathbf{A}, \mathbf{b})$  and objective coefficient  $\mathbf{c}$

**Require:** diffusion model  $\mathbf{f}_\theta$  and solution decoder  $\mathbf{d}_\theta$ .

```

1:  $\mathbf{z}_x^{(T)} \sim \mathcal{N}(\mathbf{0}, \mathbf{I})$ 
2: for  $t$  from  $T$  to 1 do
3:    $\boldsymbol{\mu} \leftarrow \frac{\sqrt{\bar{\alpha}_t}(1-\bar{\alpha}_{t-1})}{1-\bar{\alpha}_t} \mathbf{z}_x^{(t)} + \frac{\sqrt{\bar{\alpha}_{t-1}}\beta_t}{1-\bar{\alpha}_t} \mathbf{f}_\theta(\mathbf{z}_x^{(t)}, \mathbf{z}_i, t)$ 
4:    $\boldsymbol{\Sigma} \leftarrow \Sigma_\theta(\mathbf{z}_x^{(t-1)} | \mathbf{z}_x^{(t)}, \mathbf{z}_i)$ 
5:    $\boldsymbol{\mu} \leftarrow \boldsymbol{\mu} - s \nabla_{\mathbf{z}_x^{(t)}} \left( (1-\gamma)c_\phi(\mathbf{z}_x^{(t)}, \mathbf{z}_i, \mathbf{A}, \mathbf{b}) + \gamma o_\phi(\mathbf{z}_x^{(t)}, \mathbf{z}_i, \mathbf{c}) \right)$ 
6:    $\mathbf{z}_x^{(t-1)} \sim \mathcal{N}(\boldsymbol{\mu}, \boldsymbol{\Sigma})$ 
7: end for
8: return  $\mathbf{d}_\phi(\mathbf{z}_x^{(0)}, \mathbf{z}_i)$ .
```

---

## 4.2 Non-Markovian IP Guided Sampling

For the non-Markovian sampling scheme as used in DDIM, the method for conditional sampling is no longer invalid. To guide the sampling process, existing studies [4, 10] used the score-based conditioning trick from Song et al. [34] to construct a new epsilon prediction. We found that this trick turns out ineffective in our problem setting, possibly due to unique difficulties of finding feasible solutions in IP instances.

Instead, we find that adding a direction that guides the predicted solution to constraint region in each step of reverse process helps generate more reasonable solutions. Specifically, we first generate the predicted noise according to  $\hat{\mathbf{z}}_x^{(0)} = \mathbf{f}_\theta(\mathbf{z}_x^{(t)}, \mathbf{z}_i, t)$ ,  $\boldsymbol{\epsilon}_\theta^{(t)} = \frac{\mathbf{z}_x^{(t)} - \sqrt{\bar{\alpha}_t} \hat{\mathbf{z}}_x^{(0)}}{\sqrt{1-\bar{\alpha}_t}}$ . According to (2), the transition equation of DDIM for  $\mathbf{z}_x^{(t-1)}$  from a sample  $\mathbf{z}_x^{(t)}$  can be written as

$$\mathbf{z}_x^{(t-1)} = \sqrt{\bar{\alpha}_t} \mathbf{f}_\theta(\mathbf{z}_x^{(t)}, \mathbf{z}_i, t) + \sqrt{1 - \bar{\alpha}_{t-1} - \sigma_t^2} \boldsymbol{\epsilon}_\theta^{(t)} + \sigma_t \boldsymbol{\epsilon}_t. \quad (8)$$

where the first term is the prediction of  $\mathbf{z}_x^{(0)}$  and the second term is the direction pointing to  $\mathbf{z}_x^{(t)}$ . To consider constraints in (1), we modify  $\boldsymbol{\epsilon}_\theta^{(t)}$  by adding the direction of minimizing sum of constraint violation, that is

$$\hat{\boldsymbol{\epsilon}}_\theta^{(t)} = \boldsymbol{\epsilon}_\theta^{(t)} - s \nabla_{\mathbf{z}_x^{(t)}} c_\phi(\mathbf{z}_x^{(t)}, \mathbf{z}_i, \mathbf{A}, \mathbf{b}), \quad (9)$$

where  $s$  is gradient scale. By replacing  $\boldsymbol{\epsilon}_\theta^{(t)}$  in (8) with  $\hat{\boldsymbol{\epsilon}}_\theta^{(t)}$ , we obtain *Non-Markovian Constraint Guided Sampling*, which guides the solution generated in each transition to approach constraint region. Equivalently, it is to perform a gradient descent step with a step-size shrinking to zero as  $t \rightarrow 0$  when  $\sigma_t \rightarrow 0$ . To further consider the objective function together with the constraint, we can update  $\boldsymbol{\epsilon}_\theta^{(t)}$  as follows:

$$\hat{\boldsymbol{\epsilon}}_\theta^{(t)} = \boldsymbol{\epsilon}_\theta^{(t)} - s \nabla_{\mathbf{z}_x^{(t)}} \left( (1-\gamma)c_\phi(\mathbf{z}_x^{(t)}, \mathbf{z}_i, \mathbf{A}, \mathbf{b}) + \gamma o_\phi(\mathbf{z}_x^{(t)}, \mathbf{z}_i, \mathbf{c}) \right), \quad (10)$$

where  $\gamma \in [0, 1]$  is the leverage factor for balancing constraint and objective. This method is called *Non-Markovian IP Guided Diffusion Sampling*, as presented in Algorithm 3.

---

**Algorithm 3** Non-Markovian IP Guided Diffusion Sampling
 

---

**Input:** gradient scale  $s$ , leverage factor  $\gamma$ , constraint information  $(\mathbf{A}, \mathbf{b})$  and objective coefficient  $\mathbf{c}$

**Require:** diffusion model  $\mathbf{f}_\theta$ , solution decoder  $\mathbf{d}_\theta$

```

1:  $\mathbf{z}_x^{(T)} \sim \mathcal{N}(\mathbf{0}, \mathbf{I})$ 
2: for  $t$  from  $T$  to 1 do
3:    $\boldsymbol{\epsilon}_\theta^{(t)} \leftarrow (\mathbf{z}_x^{(t)} - \sqrt{\bar{\alpha}_t} \mathbf{f}_\theta(\mathbf{z}_x^{(t)}, \mathbf{z}_i, t)) / \sqrt{1 - \bar{\alpha}_t}$ 
4:    $\hat{\boldsymbol{\epsilon}}_\theta^{(t)} \leftarrow \boldsymbol{\epsilon}_\theta^{(t)} - s \nabla_{\mathbf{z}_x^{(t)}} \left( (1-\gamma)c_\phi(\mathbf{z}_x^{(t)}, \mathbf{z}_i, \mathbf{A}, \mathbf{b}) + \gamma o_\phi(\mathbf{z}_x^{(t)}, \mathbf{z}_i, \mathbf{c}) \right)$ 
5:    $\mathbf{z}_x^{(t-1)} \leftarrow \sqrt{\bar{\alpha}_t} \mathbf{f}_\theta(\mathbf{z}_x^{(t)}, \mathbf{z}_i, t) + \sqrt{1 - \bar{\alpha}_{t-1} - \sigma_t^2} \hat{\boldsymbol{\epsilon}}_\theta^{(t)} + \sigma_t \boldsymbol{\epsilon}_t$ 
6: end for
7: return  $\mathbf{d}_\phi(\mathbf{z}_x^{(0)}, \mathbf{z}_i)$ .
```

---

## 5 Experiments

This section empirically investigates the effectiveness of our method in solving IP instances. The efficacy is evaluated with two metrics: *feasible ratio* and *objective value*. The feasible ratio measures the proportion of feasible solutions among all sampled solutions and the objective value obtained from the generated feasible solutions measures the solution quality. Additionally, we also present gap between feasible solution  $x$  and optimal solution  $x^*$  via  $\frac{|c^T(x-x^*)|}{\max(|c^T x|, |c^T x^*|)}$  for comparing the performance more clearly.

We evaluate our methods on four IP datasets generated by the Ecolib library [26]:

- *Set Cover (SC)* is to find the least number of subsets that cover a given universal set.
- *Capacitated Facility Location (CF)* is to locate a number of facilities to serve the sites with a given demand and the aim is minimize the total cost.
- *Combinatorial Auction (CA)* is to help bidders place unrestricted bids for bundles of goods and the aim is to maximize the revenue.
- *Independent Set (IS)* is to find the maximum subset of nodes of an undirected graph such that no pair of nodes are connected.

We compare the performance of our approach with state-of-the-art methods including Neural Diving (ND) [21], the Predict-and-Search algorithm (PS) [8], and heuristic solutions from SCIP 8.0.1 [3] and Gurobi 9.5.2 [7]. Detailed descriptions of the datasets and baseline methods are provided in Appendix A.3. Moreover, we incorporate the best objective values, which serve as the ground truth, acquired by executing Gurobi on each instance for a duration of 100 seconds. To ensure clarity, we use *IP Guided DDPM* to denote the (Markovian) IP Guided Diffusion sampling in Section 4.1, and *IP Guided DDIM* to represent the Non-Markovian IP Guided Diffusion sampling in Section 4.2.

In the following, we first illustrate the guided diffusion sampling and emphasize its distinctions to Neural Diving and vanilla generation process in diffusion models in Section 5.1. Further, we evaluate the feasibility and quality of solutions generated by IP guided DDIM across all four datasets in Section 5.2. Furthermore, we conduct

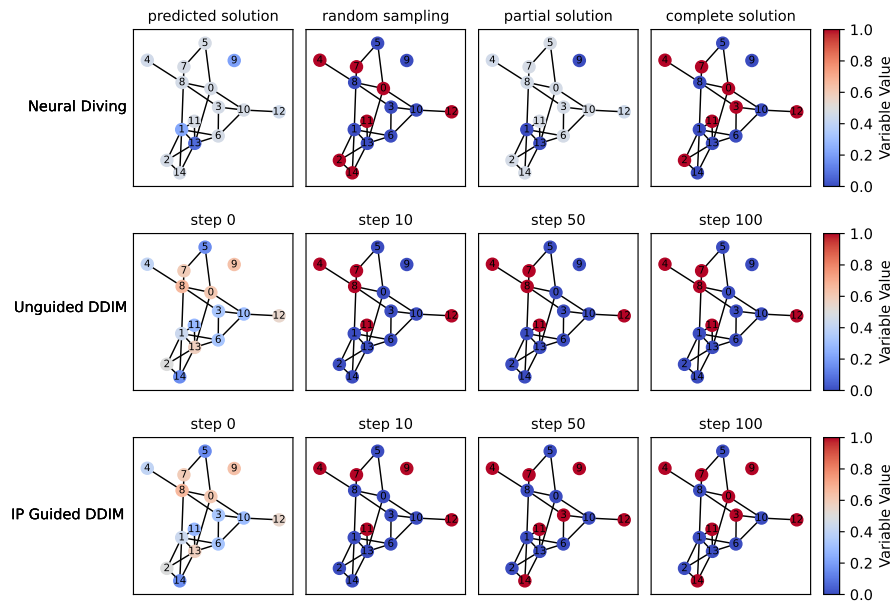


**Figure 3: The sampling results from different methods.** For Neural Diving, we present the predicted solution from GCN, random sampling according to the predicted solution, the partial solution obtained via SelectiveNet (only node 1, 9 and 13 are assigned to 0), and the completing result by calling CompleteSol heuristic. For DDIM and IP Guided DDIM, we present the results from different time steps (transformed to solution space by a decoder) during sampling.

an ablation study to investigate the impact of different guided approaches and contrastive learning in Section 5.3. In Section 5.4, we demonstrate the scalability of our approach by applying it to larger instances and present the outcomes of qualitative analysis of solutions. All experiments are performed in a workstation with two Intel(R) Xeon(R) Platinum 8163 CPU @ 2.50GHz, 176GB ram and two Nvidia V100 GPUs. We also provide the total training and inference time in Appendix A.5. The detailed hyper-parameters for IP guided sampling can be found in Appendix A.6. The codes can be found in: <https://github.com/agent-lab/diffusion-integer-programming>.

## 5.1 Illustrative experiments

The maximal independent set problem involves finding the largest subset of nodes in an undirected graph where no two nodes are connected. We focus on an illustrative example: a graph consisting of 15 nodes and 22 edges. This graph can be transformed into an integer programming (IP) instance with 15 variables and 22 constraints. The graph is depicted in Figure 3, and we present the results from Neural Diving, and from the different time steps of unguided DDIM and IP Guided DDIM. Among the three algorithms, Neural Diving fixes only three node values and uses the Completesol heuristic to find an independent set containing seven nodes. However, the random sampling solution based on predicted probability from Neural Diving is infeasible. Unguided DDIM is unable to find a feasible solution (there is an edge between node 7 and node 8). In contrast, IP Guided DDIM is able to fetch the optimal solution by finding an independent set containing eight nodes during the sampling process, where no two nodes are connected. Notably, the quality

of the solution improves as the sampling process progresses. The independent set contains 5 nodes at step 10, 7 nodes at step 50, and finally 8 nodes (the optimal solution) at step 100. These indicate that IP Guided DDIM outperforms Neural Diving and Unguided DDIM in finding the optimal solution for this illustrative example.

## 5.2 Performance Evaluation

In this section, we evaluate the performance of different methods by comparing their average feasible ratios, gaps and average objective values across four datasets mentioned earlier. Each dataset contains 100 instances. For each instance, we sample 30 solutions and calculate the corresponding metrics, which allows us to assess the performance of each method in terms of both solution feasibility and objective value across the different datasets.

We first compare the feasibility ratio of the *complete* solutions generated by IP Guided Diffusion with the *partial* solutions generated by Neural Diving, due to the inability of Neural Diving to produce complete solutions. In Neural Diving, the expected proportion of variables assigned by the model is controlled by the hyper-parameter "Coverage"  $C$ . A higher  $C$  results in more variables being assigned by the model, which generally leads to a lower feasibility ratio. Therefore, a carefully prescribed coverage  $C$  is crucial in Neural Diving to ensure the feasibility of partial solutions. In this experiment, we trained two variants of Neural Diving with different coverage thresholds for each dataset. For the SC, CA, and IS datasets, the coverage are set to 0.2 (low coverage) and 0.3 (high coverage) respectively. However, for the CF dataset, the coverage

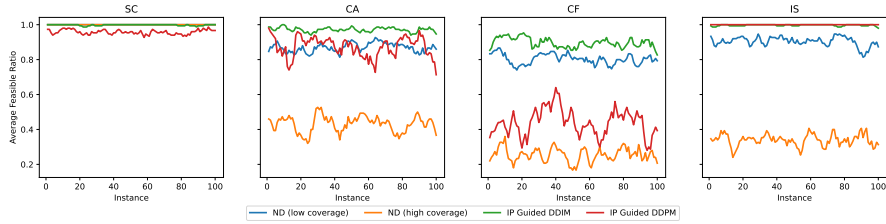


Figure 4: The feasible ratio in 100 instances, with each instance sampled 30 complete or partial solutions. For diffusion model, we measure the feasible ratio of complete solutions. Two versions of Neural Diving are trained with distinct coverage thresholds, referred to as ND (low coverage) and ND (high coverage). The feasibility ratio is evaluated only for partial solutions from Neural Diving, as the complete solutions from this method yield a 0% feasibility ratio.

Table 1: The average objective value (obj.), gap and feasible ratio (fea.) for 100 instances on 4 datasets. Optimal, heuristic, complete and partial denote optimal solutions from Gurobi, heuristic solutions from solvers, complete solutions from models, and partial solutions from models. CompleteSol and search indicates the CompleteSol heuristic and predict-and-search algorithm for completing the partial solutions, respectively.

Algorithm	Solutions' Type	SC (min)			CF (min)			CA (max)			IS (max)		
		obj.	gap	fea.	obj.	gap	fea.	obj.	gap	fea.	obj.	gap	fea.
Gurobi (100s)	Optimal	168.3	0.0%	100%	11405.5	0.0%	100%	36102.6	0.0%	100%	685.3	0.0%	100%
SCIP	Heuristic	1967.0	91.4%	<b>100%</b>	84748.4	86.5%	<b>100%</b>	28007.4	22.4%	<b>100%</b>	447.8	34.7%	<b>100%</b>
Gurobi	Heuristic	<b>522.4</b>	<b>67.8%</b>	<b>100%</b>	50397.3	77.4%	<b>100%</b>	<b>30052.0</b>	16.8%	<b>100%</b>	415.5	39.4%	<b>100%</b>
Neural Diving	Complete	-	-	0.0%	-	-	0.0%	-	-	0.0%	-	-	0.0%
IP Guided DDPM (Ours)	Complete	577.9	70.8%	95.7%	58488.1	80.5%	44.0%	800.3	97.8%	87.3%	129.9	81.0%	<b>100%</b>
IP Guided DDIM (Ours)	Complete	533.5	68.5%	99.8%	<b>25119.2</b>	<b>54.6%</b>	89.7%	26916.9	25.4%	97.1%	<b>455.6</b>	<b>33.5%</b>	99.7%
Neural Diving	Partial + CompleteSol	849.0	80.2%	<b>100%</b>	14259.8	20.0%	81.3%	30143.6	16.5%	87.0%	484.1	29.4%	90.4%
PS	Partial + Search	593.7	71.7%	<b>100%</b>	32119.8	64.5%	<b>100%</b>	31159.5	13.7%	<b>100%</b>	587.9	14.2%	<b>100%</b>
IP Guided DDIM (Ours)	Partial + CompleteSol	<b>255.5</b>	<b>34.1%</b>	<b>100%</b>	<b>14224.1</b>	<b>19.8%</b>	<b>100%</b>	<b>32491.1</b>	<b>10.0%</b>	99.7%	<b>639.4</b>	<b>6.7%</b>	<b>100%</b>

Table 2: Ablation study for 100 instances on 4 datasets with different guidances.

dataset	Unguided DDIM		Constraint Guided DDIM		Objective Guided DDIM		IP Guided DDIM w/o CISP		IP Guided DDIM	
	obj.	fea.	obj.	fea.	obj.	fea.	obj.	fea.	obj.	fea.
SC (min)	-	0.0%	63046.9	<b>99.8%</b>	-	0.0%	763.4	99.8%	<b>533.5</b>	<b>99.8%</b>
CF (min)	-	0.0%	53311.2	74.1 %	-	0.0%	31319.8	41.7%	<b>25119.2</b>	<b>89.7%</b>
CA (max)	-	0.0%	5157.2	<b>99.7%</b>	-	0.0%	23383.3	57.7%	<b>26916.9</b>	97.1 %
IS (max)	-	0.0%	386.5	<b>100 %</b>	-	0.0%	<b>479.1</b>	68.9%	455.6	99.7%

thresholds are set to 0.1 and 0.2. Figure 4 presents the average feasible ratio for 100 instances. In this comparison, the feasible ratio of complete solutions from IP guided DDIM outperforms the solutions of Neural Diving in almost all instances.

To more comprehensively evaluate the performance of the diffusion model, we compare it against different baselines in Table 1. For SCIP, we adopt the first solution obtained through non-trivial heuristic algorithms during the solving phase. For Gurobi, we use the best heuristic solution for each instance as a benchmark. Additionally, we include the optimal objective values (obtained through running Gurobi for 100 seconds on each instance) as ground-truth. For Neural Diving, complete solutions are frequently infeasible. As such, we employ a low-coverage model that prioritizes the feasibility of partial solutions. Subsequently, a CompleteSol heuristic is

utilized to finalize these partial solutions. In the case of the Predict and Search algorithm (PS), we construct a trust region using partial solutions with the same proportion of assigned variables as Neural Diving and use Gurobi as the Solver to search the best heuristic solutions found as a benchmark. To ensure a fair comparison, we report not only the quality of the complete solutions generated by our methods (IP Guided DDIM/DDPM), but also the quality of partial solutions. For this, we randomly select the same proportion of variables from DDIM's complete solutions as the ratio from Neural Diving and PS as our partial solutions. We then use the CompleteSol heuristic to finalize these partial solutions.

The results are presented in Table 1. It is evident that the complete solutions produced using the IP Guided DDIM method have a

**Table 3: The average objective value (obj.), gap and the feasible ratio (fea.) for 100 instances in 3 different size SC datasets. Optimal, heuristic, complete and partial denote optimal solutions from Gurobi, heuristic solutions from solvers, complete solutions from models, and partial solutions from models. CompleteSol and search indicates CompleteSol heuristic and predict-and-search algorithm for completing the partial solutions, respectively.**

Algorithm	Solutions' Type	SC (2000)			SC (3000)			SC (4000)		
		obj.	gap	fea.	obj.	gap	fea.	obj.	gap	fea.
Gurobi (100s)	Optimal	168.3	0.0%	100%	140.4	0.0%	100%	126.9	0.0%	100%
SCIP	Heuristic	1977.0	91.4%	100%	2236.2	93.7%	<b>100%</b>	2386.0	94.7%	<b>100%</b>
Gurobi	Heuristic	522.4	67.8%	100%	718.8	80.5%	<b>100%</b>	1454.5	91.3%	<b>100%</b>
Neural Diving	Complete	-	-	0.0%	-	-	0.0%	-	-	0.0%
IP Guided DDPM (Ours)	Complete	594.7	70.8%	96.5%	<b>451.8</b>	<b>68.9%</b>	83.7%	<b>440.7</b>	<b>71.2%</b>	77.9%
IP Guided DDIM (Ours)	Complete	<b>533.5</b>	<b>68.5%</b>	99.8%	486.8	71.2%	99.9%	464.9	72.7%	<b>100%</b>
Neural Diving	Partial + CompleteSol	849.0	80.2%	<b>100%</b>	1145.8	87.7%	<b>100%</b>	1465.6	91.3%	<b>100%</b>
PS	Partial + Search	593.7	71.7%	<b>100%</b>	737.0	80.9%	<b>100%</b>	994.9	87.2%	<b>100%</b>
IP Guided DDIM (Ours)	Partial + CompleteSol	<b>255.5</b>	<b>34.1%</b>	<b>100%</b>	<b>217.4</b>	<b>35.4%</b>	<b>100%</b>	<b>195.9</b>	<b>35.2%</b>	<b>100%</b>

feasible ratio of at least 89.7%, and their objective values are comparable to the best heuristic solutions from Gurobi. In contrast, the complete solutions obtained solely through Neural Diving are consistently infeasible. Moreover, the integration of partial solutions from IP Guided DDIM with the CompleteSol heuristic outstrips that of all methods in terms of objective values. This improvement is demonstrated by a 3.7 to 33.7% reduction in the gap to optimal values, while the feasibility ratio for all datasets approaches 100%.

### 5.3 Ablation Study

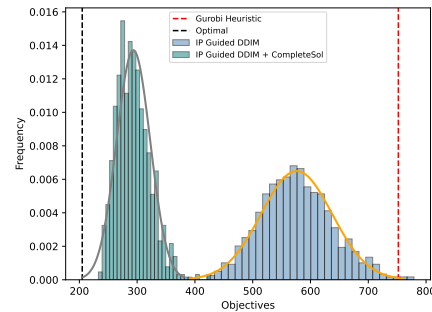
We ablate on unguided DDIM (with  $s = 0$ ), constraint guided DDIM (with  $\gamma = 1$ ), objective guided DDIM (with  $\gamma = 0$ ) models and IP guided DDIM on four datasets. We also include an experiment where we train IP and solution embeddings directly via algorithm 1 without CISP, in order to assess the advantages of contrastive learning, i.e. IP Guided DDIP w/o CISP in Table 2. The results are presented in Table 2. Evidently, the constraint guidance is crucial in generating feasible solutions, and the objective guidance further enhances the quality of solutions. Moreover, the experiments demonstrate that CISP plays a crucial role in ensuring that the solutions produced by our methods are more feasible. Therefore, combining both constraint and objective guidance achieves good quality solutions with high probability.

### 5.4 Scalability test and qualitative analysis

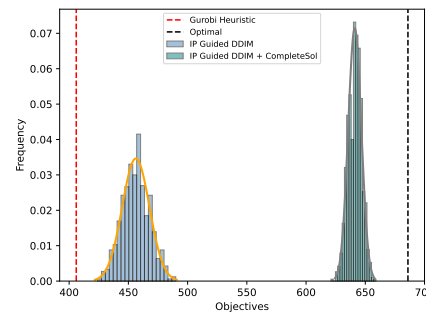
Practitioners often aim to apply the models learned to solve problems of larger scales than the ones used for data collection and training. To estimate how well a model can generalize to bigger instances, we evaluate its performance on datasets of varying sizes from the Set Cover problem (minimization problem). We utilize three size categories:

- SC (2000): 2000 variables, 1000 constraints
- SC (3000): 3000 variables, 1500 constraints
- SC (4000): 4000 variables, 2000 constraints

It is worth noting that all models were trained using the SC (2000) dataset. The results in table 3 demonstrate that IP guided DDPM consistently performs well across all three different-sized datasets, indicating that our framework possesses strong generalization capabilities.



(a) SC instance (minimization).



(b) IS instance (maximization).

**Figure 5: The objective distribution of 1000 solutions sampled from a single instance.**

Diffusion models are generative models that capture the distribution of a dataset. In this experiment, we focus on the distribution of solutions generated by our methods. We take a single instance from the SC dataset and IS dataset and use the IP Guided DDIM algorithm to generate 1000 complete feasible solutions. We also randomly sample 20% of variable values from each solution and



use the CompleteSol heuristic to fill in the remaining variables. We analyze the distribution of objective values for these complete solutions and compare them with the optimal objective values and the best heuristic solutions found by the Gurobi heuristic. The results are shown in Figure 5. Clearly, the complete solutions directly generated by the IP Guided DDIM algorithm are superior to the best solutions from the Gurobi heuristic. Furthermore, the objective values from the partial solutions completed by the CompleteSol heuristic are closer to the optimal value.

## 6 Related Work

We start the related work section with a summary of deep learning techniques used in the construction of feasible solutions for Integer Programming (IP) problems. Gasse et al. [5] propose a method that combines a bipartite graph with a Graph Convolutional Network (GCN) to extract representations of Integer Programming (IP) instances. Although this approach is primarily employed to learn the branching policy in the branch and bound algorithm, it is worth noting that this modeling method can also be utilized for the prediction of solutions for IP instances. However, the solutions produced by GCN directly are often infeasible or sub-optimal. To address this, Neural Diving [21] leverages the SelectiveNet [6] to assign values to only a subset of the variables based on a coverage threshold, with the rest of the variables being completed via an IP Solver. To further improve the feasibility of generated solutions, Han et al. [8] proposes a predict-search framework that combines the predictions from GNN model with trust region method. However, this method still relies on IP solver to solve a modified instance (adding neighborhood constraints to origin instance) in order to get complete solutions. Similar to Nair et al. [21], Khalil et al. [14] integrate GNN into integer programming solvers and apply it to construct a partial solutions through a prescribed rounding threshold, which is then completed using SCIP. In contrast, our method aims to learn the latent structure of IP instances by diffusion models, and obtains complete feasible solutions through guided diffusion sampling, without any reliance on the IP solver.

Another set of related works to our paper is diffusion models [9, 32]. As the latest state-of-the-art family of deep generative models, diffusion models have demonstrated their ability to enhance performance across various generative tasks [37]. In this paper, we focus our discussion specifically on conditional diffusion models. Unlike unconditional generation, conditional generation emphasizes application-level contents as a condition to control the generated results based on predefined intentions. To enable this conditioning, Dhariwal and Nichol [4] introduce the concept of classifier guidance, which enhances sample quality by conditioning the generative process on an additional trained classifier. In the same vein, Ho and Salimans [10] propose a joint training strategy for both conditional and unconditional diffusion models, i.e., classifier-free guidance. This approach combines the resulting conditional and unconditional scores to achieve a balance between sample quality and diversity. This idea has also found its effectiveness in Topology Optimization [20]. We thus take a similar derivation from the classifier guidance and devise IP-guided diffusion sampling by incorporating the objectives and constraints into the transition probability.

## 7 Discussions

### 7.1 The Importance of Solution Generation

Integer Programming solvers typically rely on branch-and-bound or branch-and-cut algorithms to tackle problems, often starting with a primal heuristic to find a good initial feasible solution. A robust starting solution generally accelerates the entire solving process. Our method demonstrates that diffusion models are capable of generating complete feasible solutions that satisfy all constraints. These generated solutions exhibit competitive performance compared to the heuristics employed in optimization tools such as Gurobi. Notably, the ability to generate complete solutions from scratch distinguishes our model from other neural-based approaches like Neural Diving [21] and the Predict-Search algorithm [8]. Moreover, generating feasible solutions end-to-end is especially important, as it represents a significant leap toward developing a purely neural-based method for integer programming. The paper shows that diffusion models can produce solutions that satisfy all constraints, which lays the foundation for future research in which neural networks could potentially solve such problems without relying on traditional solvers or heuristics.

### 7.2 Sampling Efficiency

The sampling time is a notable limitation of current diffusion models. Specifically, our method requires 100 iterative denoising steps for DDIM and 1000 for DDPM, resulting in longer times to generate a single solution compared to other methods. To address this issue, there have been active studies focused on accelerating diffusion sampling, such as model quantization (Li et al. [17]) and distillation (HUANG et al. [11]). These techniques can be readily integrated into our methods. Moving forward, we will enhance our method by incorporating these acceleration techniques.

## 8 Conclusion

In this paper, we presented a comprehensive framework for generating feasible solutions for Integer Programming (IP) problems. We utilized the CISP approach to establish a link between IP instances and their corresponding solutions, allowing to obtain IP embeddings and solution embeddings. To effectively capture the distribution of feasible solutions, we leveraged diffusion models, which are known for their powerful learning capabilities, to learn the distribution of solution embeddings. We further employed a solution decoder to reconstruct the solutions from their embeddings. Importantly, we proposed an IP guided sampling algorithm that explicitly incorporates the objective and constraint information to generate high-quality solutions. The experimental results on four distinct datasets demonstrate the superiority of our approach to the state-of-the-art.

## ACKNOWLEDGMENTS

Mingfei Sun is affiliated with Centre for AI Fundamentals. He is also a member of AI Hub in Generative Models, funded by Engineering and Physical Sciences Research Council (EPSRC), part of UK Research and Innovation (UKRI),

## REFERENCES

- [1] Tomer Amit, Eliya Nachmani, Tal Shaharabany, and Lior Wolf. 2021. SegDiff: Image Segmentation with Diffusion Probabilistic Models. *CoRR abs/2112.00390* (2021). arXiv:2112.00390 <https://arxiv.org/abs/2112.00390>
- [2] Reza Bayat. 2023. A Study on Sample Diversity in Generative Models: GANs vs. Diffusion Models. <https://openreview.net/forum?id=BQpCuJoMykZ>
- [3] Ksenia Bestuzheva, Mathieu Besançon, Wei-Kun Chen, Antonia Chmiela, Tim Donkiewicz, Jasper van Doornmalen, Leon Eifler, Oliver Gaul, Gerald Gamrath, Ambros Gleixner, et al. 2023. The SCIP optimization suite 8.0. *ACM Trans. Math. Softw.* 49, 2 (2023), 22:1–22:21. <https://doi.org/10.1145/3585516>
- [4] Prafulla Dhariwal and Alexander Nichol. 2021. Diffusion models beat gans on image synthesis. *Advances in neural information processing systems* 34 (2021), 8780–8794.
- [5] Maxime Gasse, Didier Chételat, Nicola Ferroni, Laurent Charlin, and Andrea Lodi. 2019. Exact combinatorial optimization with graph convolutional neural networks. *Advances in Neural Information Processing Systems* 32 (2019).
- [6] Yonatan Geifman and Ran El-Yaniv. 2019. Selectivenet: A deep neural network with an integrated reject option. In *International conference on machine learning*. PMLR, 2151–2159.
- [7] LLC Gurobi Optimization. 2021. Gurobi optimizer reference manual.
- [8] Qingyu Han, Linxin Yang, Qian Chen, Xiang Zhou, Dong Zhang, Akang Wang, Ruoyu Sun, and Xiaodong Luo. 2023. A GNN-Guided Predict-and-Search Framework for Mixed-Integer Linear Programming. In *International Conference on Learning Representations*. <https://openreview.net/forum?id=pHMpgT5xWaE>
- [9] Jonathan Ho, Ajay Jain, and Pieter Abbeel. 2020. Denoising diffusion probabilistic models. *Advances in neural information processing systems* 33 (2020), 6840–6851.
- [10] Jonathan Ho and Tim Salimans. 2022. Classifier-Free Diffusion Guidance. *CoRR abs/2207.12598* (2022). <https://doi.org/10.48550/arXiv.2207.12598> arXiv:2207.12598
- [11] JUNWEI HUANG, Zhiqing Sun, and Yiming Yang. 2023. Accelerating Diffusion-based Combinatorial Optimization Solvers by Progressive Distillation. In *ICML 2023 Workshop: Sampling and Optimization in Discrete Space*. <https://openreview.net/forum?id=AbMj31okE4>
- [12] Naoki Katoh and Toshihide Ibaraki. 1998. Resource allocation problems. *Handbook of Combinatorial Optimization: Volume 1–3* (1998), 905–1006.
- [13] James E Kelley, Jr. 1960. The cutting-plane method for solving convex programs. *Journal of the society for Industrial and Applied Mathematics* 8, 4 (1960), 703–712.
- [14] Elias B Khalil, Christopher Morris, and Andrea Lodi. 2022. Mip-gnn: A data-driven framework for guiding combinatorial solvers. In *Proceedings of the AAAI Conference on Artificial Intelligence*, Vol. 36. 10219–10227.
- [15] Diederik P. Kingma and Jimmy Ba. 2015. Adam: A Method for Stochastic Optimization. In *3rd International Conference on Learning Representations, ICLR 2015, San Diego, CA, USA, May 7–9, 2015, Conference Track Proceedings*, Yoshua Bengio and Yann LeCun (Eds.). <http://arxiv.org/abs/1412.6980>
- [16] Eugene L Lawler and David E Wood. 1966. Branch-and-bound methods: A survey. *Operations research* 14, 4 (1966), 699–719.
- [17] Xiuyu Li, Yijiang Liu, Long Lian, Huanrui Yang, Zhen Dong, Daniel Kang, Shanghang Zhang, and Kurt Keutzer. 2023. Q-Diffusion: Quantizing Diffusion Models. In *Proceedings of the IEEE/CVF International Conference on Computer Vision (ICCV)*. 17535–17545.
- [18] Ilya Loshchilov and Frank Hutter. 2019. Decoupled Weight Decay Regularization. In *7th International Conference on Learning Representations, ICLR 2019, New Orleans, LA, USA, May 6–9, 2019*. OpenReview.net. <https://openreview.net/forum?id=Bkg6RiCqY7>
- [19] Stephen J Maher, Tobias Fischer, Tristan Gally, Gerald Gamrath, Ambros Gleixner, Robert Lion Gottwald, Gregor Hendel, Thorsten Koch, Marco Lübbecke, Matthias Miltenberger, et al. 2017. The SCIP optimization suite 4.0. (2017).
- [20] François Mazé and Faez Ahmed. 2023. Diffusion models beat gans on topology optimization. In *Proceedings of the AAAI Conference on Artificial Intelligence (AAAI), Washington, DC*.
- [21] Vinod Nair, Sergey Bartunov, Felix Gimeno, Ingrid Von Glehn, Pawel Lichocki, Ivan Lobo, Brendan O’Donoghue, Nicolas Sonnerat, Christian Tjandraatmadja, Pengming Wang, et al. 2020. Solving mixed integer programs using neural networks. *arXiv preprint arXiv:2012.13349* (2020).
- [22] Alexander Quinn Nichol and Prafulla Dhariwal. 2021. Improved denoising diffusion probabilistic models. In *International Conference on Machine Learning*. PMLR, 8162–8171.
- [23] CC Pantelides, MJ Realf, and N Shah. 1995. Short-term scheduling of pipeless batch plants. *Chemical engineering research & design* 73, 4 (1995), 431–444.
- [24] David Pisinger and Stefan Ropke. 2019. Large neighborhood search. *Handbook of metaheuristics* (2019), 99–127.
- [25] Yves Pochet and Laurence A Wolsey. 2006. *Production planning by mixed integer programming*. Vol. 149. Springer.
- [26] Antoine Prouvost, Justin Dumouchelle, Lara Scavuzzo, Maxime Gasse, Didier Chételat, and Andrea Lodi. 2020. Ecole: A gym-like library for machine learning in combinatorial optimization solvers. *arXiv preprint arXiv:2011.06069* (2020).
- [27] Alec Radford, Jong Wook Kim, Chris Hallacy, Aditya Ramesh, Gabriel Goh, Sandhini Agarwal, Girish Sastry, Amanda Askell, Pamela Mishkin, Jack Clark, et al. 2021. Learning transferable visual models from natural language supervision. In *International conference on machine learning*. PMLR, 8748–8763.
- [28] Aditya Ramesh, Prafulla Dhariwal, Alex Nichol, Casey Chu, and Mark Chen. 2022. Hierarchical text-conditional image generation with clip latents. *arXiv preprint arXiv:2204.06125* 1, 2 (2022), 3.
- [29] Tadeusz Sawik. 2011. *Scheduling in supply chains using mixed integer programming*. John Wiley & Sons.
- [30] Edward Allen Silver, David F Pyke, Rein Peterson, et al. 1998. *Inventory management and production planning and scheduling*. Vol. 3. Wiley New York.
- [31] Jascha Sohl-Dickstein, Eric Weiss, Niru Maheswaranathan, and Surya Ganguli. 2015. Deep unsupervised learning using nonequilibrium thermodynamics. In *International conference on machine learning*. PMLR, 2256–2265.
- [32] Kihyuk Sohn, Honglak Lee, and Xinchen Yan. 2015. Learning structured output representation using deep conditional generative models. *Advances in neural information processing systems* 28 (2015).
- [33] Jiaming Song, Chenlin Meng, and Stefano Ermon. 2021. Denoising Diffusion Implicit Models. In *9th International Conference on Learning Representations, ICLR 2021, Virtual Event, Austria, May 3–7, 2021*. OpenReview.net. <https://openreview.net/forum?id=St1giarCHLP>
- [34] Yang Song, Jascha Sohl-Dickstein, Diederik P. Kingma, Abhishek Kumar, Stefano Ermon, and Ben Poole. 2021. Score-Based Generative Modeling through Stochastic Differential Equations. In *9th International Conference on Learning Representations, ICLR 2021, Virtual Event, Austria, May 3–7, 2021*. OpenReview.net. <https://openreview.net/forum?id=PxTIG12RRHS>
- [35] Paolo Toth and Daniele Vigo. 2002. *The vehicle routing problem*. SIAM.
- [36] L.A. Wolsey. 1998. *Integer Programming*. Wiley. <https://books.google.co.uk/books?id=x7RvQgAACAAJ>
- [37] Ling Yang, Zhilong Zhang, Yang Song, Shenda Hong, Runsheng Xu, Yue Zhao, Yingxia Shao, Wentao Zhang, Ming-Hsuan Yang, and Bin Cui. 2022. Diffusion Models: A Comprehensive Survey of Methods and Applications. *CoRR abs/2209.00796* (2022). <https://doi.org/10.48550/arXiv.2209.00796> arXiv:2209.00796
- [38] Taehyun Yoon. 2022. Confidence Threshold Neural Diving. *CoRR abs/2202.07506* (2022). arXiv:2202.07506 <https://arxiv.org/abs/2202.07506>

## A Appendix

### A.1 CISP Algorithm

The study conducted by [27] underscores the substantial efficacy of contrasting pre-training in capturing multi-modal data, with particular emphasis on its application in the text-to-image transfer domain. Drawing inspiration from this seminal work, we introduce the CISP algorithm. The primary objective of CISP is to facilitate the learning of the IP Encoder  $E_I$  and the Solution Encoder  $E_X$ , as illustrated in Algorithm 4. Within the scope of our investigation, we work with a mini-batch of data comprising instances denoted as  $I$  and their corresponding solutions denoted as  $X$ . The batch’s bipartite graph representing instances  $I$  is denoted as  $G$ . We use  $\mathbf{z}_I$  and  $\mathbf{z}_X$  to denote the embeddings of instances and solutions, respectively. Notably, both  $\mathbf{z}_I$  and  $\mathbf{z}_X$  possess identical dimensions, enabling us to compute their cosine similarity. Furthermore, within the mini-batch,  $\mathbf{z}_{I,j}$  and  $\mathbf{z}_{X,k}$  denote to the  $j$ th sample in  $\mathbf{z}_I$  and the  $k$ th sample in  $\mathbf{z}_X$ , respectively. Within this conceptual framework, we leverage the matrix  $\mathbf{s} \in \mathbb{R}^{N \times N}$  to represent the similarity between  $N$  instances and  $N$  solutions. Each element  $s_{j,k}$ , where  $j, k \in \{1, \dots, N\}$ , corresponds to the logit employed in computation of the symmetric cross-entropy loss.

### A.2 Feature Descriptions For Variables Nodes, Constraint Nodes And Edges

In Table 4, we provide a description of the features that are extracted using the *Ecole* library [26] and used as IP bipartite graph representations for training the GCN model.

**Table 4: Description of the variable, constraint and edge features in our bipartite graph representations.**

	Feature	Description
Variable	type	Type(binary, integer, impl. integer, continuous) as a one-hot encoding.
	coef	Objective coefficient, normalized.
	has_lb	Lower bound indicator.
	has_ub	Upper bound indicator.
	sol_is_at_lb	Solution value equals lower bound.
	sol_is_at_ub	Solution value equals upper bound.
	sol_frac	Solution value fractionality.
	basis_status	Simplex basis status(lower, basic, upper, zero) as a one-hot encoding.
	reduced_cost	Reduced cost, normalized.
	age	LP age, normalized.
	sol_val	Solution value.
Constraint	obj_cos_sim	Cosine similarity with objective.
	bias	Bias value, normalized with constraint coefficients.
	is_tight	Tightness indicator in LP solution.
	dualsol_val	Dual solution value, normalized.
	age	LP age, normalized with total number of LPs.
Edge	coef	Constraint coefficient, normalized per constraint.

**Algorithm 4** Contrastive IP-Solution Pre-Training (CISP)

**Input:** The mini-batch size  $N$ , the mini-batch bipartite graph representations of IP instance set  $I$ , denoted by  $G$ , and corresponding mini-batch solutions  $X$

**Require:** IP Encoder  $E_I$ , Solution Encoder  $E_X$ , temperature parameter  $\tau$

- 1: Get IP and solution embeddings  $\mathbf{z}_I, \mathbf{z}_X = E_I(G), E_X(X) \ // N \times n \times d$ , where  $n$  is the padding length of variables and  $d$  is the embedding size.
- 2: **for**  $j \in \{1, 2, \dots, N\}$  and  $k \in \{1, 2, \dots, N\}$  **do**
- 3: Flatten  $\mathbf{z}_{I,j}$  and  $\mathbf{z}_{X,k}$  into vectors  $\bar{\mathbf{z}}_{I,j}$  and  $\bar{\mathbf{z}}_{X,k}$
- 4:  $\mathbf{s}_{j,k} = e^{\tau} \cdot \bar{\mathbf{z}}_{I,j}^T \bar{\mathbf{z}}_{X,k} / (\|\bar{\mathbf{z}}_{I,j}\| \|\bar{\mathbf{z}}_{X,k}\|) \ //$  compute similarity for IP and solution embeddings
- 5: **end for**
- 6: Set labels  $\mathbf{y} = (1, 2, \dots, N)$
- 7: Compute cross-entropy loss  $\mathcal{L}_I$  by utilizing  $\mathbf{s}_{j,*}$  and  $\mathbf{y}$ .
- 8: Compute cross-entropy loss  $\mathcal{L}_X$  by utilizing  $\mathbf{s}_{*,k}$  and  $\mathbf{y}$ .
- 9: Compute the symmetric loss  $\mathcal{L} = (\mathcal{L}_I + \mathcal{L}_X)/2$
- 10: **return**  $\mathcal{L}$

**A.3 Datasets and Baselines**

**A.3.1 Datasets.** For all four datasets, we randomly generate 1000 instances (800 for training, 100 for validation and 100 for testing). Table 5 summarizes the numbers of constraints, variables and problem type of each dataset. We then collect feasible solutions and their objective values for each instance by running the Gurobi [7] or SCIP [3], where the time limit is set to 1000s for each instance. For those instances with a large number of feasible solutions, we only keep 500 best solutions. We adopt the same features exacted via the Ecole library as in [5] and exclude those related to feasible solutions. The specific features are shown in Appendix A.2.

**A.3.2 Baselines.** We compared our method with the following baselines:

- *SCIP* [3] (an open source solver): SCIP is currently one of the fastest non-commercial solvers for mixed integer programming (MIP) and mixed integer nonlinear programming (MINLP). Here, we focus on comparing the quality of initial solutions with SCIP. Instead of relying on the first feasible solution generated by SCIP, which are often of low quality due to the use of trivial heuristics, we employ the first solution produced via non-trivial heuristic algorithms during the solving process of SCIP [3] (i.e. the first feasible solution after the pre-solving stage of SCIP).
- *Gurobi* [7] (the powerful commercial solver): Gurobi is a highly efficient commercial mathematical optimization solver. As our focus is on comparing feasible solutions, we consider the best solutions obtained through Gurobi’s default heuristic algorithms as a benchmark.
- *Neural Diving (ND)* [21]: Neural Diving adopts a solution prediction approach, training a GCN to predict the value of each variable. It then incorporates SelectiveNet [6] to generate partial solutions with a predefined coverage threshold  $C$  (e.g., a coverage threshold  $C = 0.2$  means that the expectation of the number of assigned variables by the neural network is 20%). This threshold is typically set to be low ( $<0.5$ ) to ensure the feasibility of partial solutions. In our experiments, to evaluate the feasibility of solutions, we set two different coverage levels, namely low coverage (which usually indicates higher feasibility) and high coverage (which usually indicates lower feasibility), for each dataset. We then compare the feasibility of the partial solutions with the complete solutions generated by our methods. To assess the quality of solutions, we employ the Completesol heuristic in SCIP (Algorithm 4 in [19]) to enhance the partial solutions. This heuristic involves solving auxiliary IP instances by fixing the

variables from the partial solutions. By utilizing this heuristic, we can obtain more complete solutions and evaluate their quality.

- *Predict-and-search algorithm (PS)* [8]: The PS algorithm, similar to Neural Diving, utilizes graph neural networks to predict the value of each variable. It then searches for the best feasible solution within a trust region constructed by the predicted partial solutions. This method requires setting parameters  $(k_0, k_1)$  to represent the numbers of 0's and 1's in a partial solution, and  $\Delta$  to define the range of the neighborhood region of the partial solution. To search a high-quality feasible solution, this method adds neighborhood constraints to origin instance, which produces modified IP instance. Therefore, an IP solver such as SCIP or Gurobi is required to solve the modified instance and obtain feasible solutions. In our experiments, we use Gurobi as the solver and control the parameters  $\Delta$  to ensure that the modified instance is 100% feasible. We considered the best heuristic solutions from the modified instance found by Gurobi as our baseline.

**Table 5: Instance size of each dataset**

Dataset	Constraints	Variables	Problem Type
SC	1000	2000	minimize
CF	5051	5050	minimize
CA	786	1500	maximize
IS	6396	1500	maximize

#### A.4 Training Details

We trained the CISP and diffusion model on four IP datasets. Each dataset contained 800 training instances, with 500 solutions collected for each instance. In each batch, we sampled 64 instances, and for each instance, we sample one solution from 500 solutions in proportion to the probability of the objective value as a possible label. This implies that solutions with better objective values had a higher probability of being sampled. We iterated through all instances (with one solution per instance) in each epoch.

For the Solution Encoder, we utilized a single transformer encode layer with a width of 128. The IP encoder adopted the architecture described in [21], using GCN to obtain embeddings for all variables as IP embeddings. Both models transformed the features of the solution and IP into latent variables with a dimension of 128, enabling convenient computation of cosine similarity in CISP. The CISP was trained using the AdamW Optimizer [18]. We employed a decreasing learning rate strategy, starting with a learning rate of 0.001 and linearly decaying it by a factor of 0.9 every 100 epochs until reaching 800 epochs. The model training was performed with a batch size of 64.

For the diffusion model, we utilized a single-layer Transformer encoder with a width of 128 to predict  $\mathbf{z}_x$  and adjusted the number of time steps to 1000. The forward process variances were set as constants, increasing linearly from  $\beta_1 = 10^{-4}$  to  $\beta_T = 0.02$ , following the default setting of DDPM [9]. The solution decoder model

was jointly trained with the diffusion model and consisted of two Transformer encode layers with a width of 128. The loss function was defined as the sum of the diffusion loss, decoder loss, and the penalty for violating constraints, as shown in (5). Here,  $\lambda$  is set to be the number of variables in the instances from the training set, excluding the IS dataset, where  $\lambda = 0$ . We trained diffusion and decoder model for 100 epochs with batch size of 32 via Adam Optimizer [15].

#### A.5 Training and Inference Time

In this section, we report the training time (including CISP pretraining and Diffusion model) for each dataset, which takes 100 epochs for both CISP and Diffusion model to converge. Additionally, we provide the total inference time for sampling 3000 solutions by using IP Guided DDIM and DDPM. From Table 6, we observe that our method requires a reasonable amount of time for model training. During the inference phase, IP Guided DDIM demonstrates faster performance compared to IP Guided DDPM with average time of 0.46s-1.68s for sampling each solution. Moreover, as shown in the experiment results from Section 5, IP Guided DDIM also achieves better performance than DDPM, making it suitable for practical applications.

**Table 6: Total training time and inference time for sampling 3000 solutions for each dataset**

Dataset	Training (CISP + Diffusion)	IP Guided DDIM	IP Guided DDPM
SC	24.4m	37.5m	374m
CF	71.7m	84m	805m
CA	9.3m	23m	233.5m
IS	11.1m	23m	234m

#### A.6 Hyperparameters for IP Guided Sampling

During the sampling process, we configured the number of steps to be 1000 for IP Guided Diffusion sampling (IP Guided DDPM) and 100 for Non-Markovian IP Guided Diffusion sampling (IP Guided DDIM). In Table 7, we provide the specific values for the gradient scale  $s$  and leverage factor  $\gamma$ .

**Table 7:  $s$  and  $\gamma$  settings in different dataset**

dataset	IP Guided DDIM		IP Guided DDPM	
	$s$	$\gamma$	$s$	$\gamma$
SC (2000)	100,000	0.9	15,000	0.1
SC (3000)	150,000	0.9	22,500	0.1
SC (4000)	200,000	0.9	30,000	0.1
CF	1,000	0.7	500,000	0.1
CA	20,000	0.7	10,000	0.3
IS	20,000	0.5	10,000	0.1